JPET Fast Forward. Published on September 2, 2014 as DOI: 10.1124/jpet.114.215152
This article has not been copyedited and formatted. The final version may differ from this version.

Title page

Prevention of Bleomycin-Induced Lung Inflammation and Fibrosis in Mice by Naproxen and JNJ7777120 Treatment

Arianna Carolina Rosa, Alessandro Pini, Laura Lucarini, Cecilia Lanzi, Eleonora Veglia, Robin L. Thurmond, Holger Stark and Emanuela Masini

Departments of Drug Science and Technology, University of Turin, Turin, Italy (A.C.R., E.V.); NEUROFARBA, Section of Pharmacology (L.L., C.L., E.M.); Experimental and Clinical Medicine (A.P.), University of Florence, 50139 Florence, Italy; Janssen Research & Development, L.L.C., San Diego, CA, USA (R.L.T) and Heinrich-Heine Düsseldorf University, Institute of Medicinal Chemistry, D40225 Düsseldorf, Germany (H.S.)

Running Title page

Running title: Effect of JNJ7777120 and naproxen on lung fibrosis in mice

Corresponding author: Emanuela Masini, MD
Department of NEUROFARBA, Section of Pharmacology,
University of Florence,
Viale G. Pieraccini n.6, 50139 Florence, Italy
Phone ++39 055 4271233
Email: emanuela.masini@unifi.it

Text pages 26

Tables 0

Figures 7

References 39

Word number

Abstract 232

Introduction 603

Discussion 1104

NONSTANDARD ABBREVATIONS: COX, cyclooxygenase; H_4R, histamine H_4 receptor; MDA, Malonyldialdehyde, MPO; myeloperoxidase; NSAID, non-steroidal anti-inflammatory drug; 8-OHdG, 8-hydroxy-2'-deoxyguanosine; PAO, pressure at the airway opening; PAS, periodic acid-Schiff; ROS, reactive oxygen species; TBARS, thiobarbituric acid-reactive substance; JNJ7777120, 1-[(5-chloro-1H-indol-2-yl)carbonyl]-4-methylpiperazine; (TGF)-β, Transforming Growth Factor; PGE_2, Prostaglandin E_2; IL_{10}, Interleukin-10

Section category: Inflammation, Immunopharmacology, and Asthma

JPET Fast Forward. Published on September 2, 2014 as DOI: 10.1124/jpet.114.215152
This article has not been copyedited and formatted. The final version may differ from this version.

ABSTRACT

Pulmonary fibrosis, a progressive and lethal lung disease characterized by inflammation and accumulation of extracellular matrix components, is one of major therapeutic challenge, where new therapeutic strategies are warranted. COX inhibitors have been previously utilized to reduce inflammation. Histamine H_4 receptor (H_4R), largely expressed in haematopoietic cells, has been identified as a novel target for inflammatory and immune disorders. The aim of this study was to evaluate the effect of JNJ7777120, a selective H_4R antagonist, and naproxen, a well-known NSAID, and their combination in a murine model of bleomycin-induced fibrosis. Bleomycin (0.05 IU) was instilled intra-tracheally to C57BL/6 mice, which were then treated by micro-osmotic pump with vehicle, JNJ7777120 (40 mg/kg/b.wt.), naproxen (21 mg/kg/b.wt.) or a combination of both. Airway resistance to inflation, an index of lung stiffness, was assessed and lung specimens were processed for inflammation, oxidative stress and fibrosis markers. Both the drugs alone were able to reduce the airway resistance to inflation induced by bleomycin and the inflammatory response by decreasing the COX-2 and MPO expression and activity and TBARS and 8-OHdG production. Lung fibrosis was inhibited as demonstrated by the reduction of tissue levels of TGF-β, collagen deposition, relative goblet cell number and smooth muscle layer thickness. Our results demonstrate that both JNJ7777120 and naproxen exert an anti-inflammatory and anti-fibrotic effect increased by their combination, which could be an effective therapeutic strategy in the treatment of pulmonary fibrosis.

JPET Fast Forward. Published on September 2, 2014 as DOI: 10.1124/jpet.114.215152
This article has not been copyedited and formatted. The final version may differ from this version.

Introduction

Pulmonary fibrosis is a disease causing considerable morbidity and mortality and it is one of the major therapeutic challenges (Hauber and Blaukovitsch, 2010; Raghu *et al.*, 2011).

The hallmark of pulmonary fibrosis is a patho-physiological response of the lungs to chronic injury and inflammation that manifests as abnormal and excessive deposition of collagen and other extracellular matrix components. Accumulation of vascular exudates and inflammatory cells within the injured alveolar space lead to epithelial cell injury. These exudates enhance the proliferation of resident fibroblasts and their trans-differentiation into myofibroblasts (activated collagen-secreting fibroblasts) as well as the transformation of epithelial cells, a typical feature of all fibrotic diseases (Kisseleva and Brenner, 2008). The myofibroblasts, organized into agglomerations of cells known as fibroblastic foci, produce an excessive tissue matrix, especially collagen, and the fibrosis becomes established. (du Bois, 2010). This results in progressive airway stiffening and thickening of the air-blood membrane, which make breathing difficult and eventually leads to respiratory failure.

Compelling evidences suggest that inflammatory cells influence fibrosis by releasing pro-fibrotic mediators (Stramer *et al*., 2007). However, there is no effective therapy available that can favourably influence the course of the disease (Hauber and Blaukovitsch, 2010; Raghu *et al.*, 2011). The use of glucocorticoids or immunosuppressive medications has been the conventional pharmacological approach, although current reviews suggest that there is no therapeutic benefit with these drugs in comparison with their significant side effects (Carter, 2011). In this context, non-steroidal antinflammatory drugs (NSAIDs), inhibiting the biosynthesis of prostanoids, have been proposed as a possible therapy in pulmonary fibrosis. Naproxen, a well-known classical NSAID, was found to be effective in reducing lung inflammation and preventing collagen accumulation in the model of bleomycin-induced lung fibrosis (Masini *et al.*, 2005; Pini *et al.*, 2012). However, the clinical relevance of NSAIDs is questioned by their ineffectiveness in improving pulmonary function or survival in patients with idiopathic pulmonary fibrosis (Davies *et*

al., 2003; Richeldi *et al.*, 2003). Our data suggest that prostaglandin biosynthesis inhibition could have favorable effects during the overt inflammatory phase of the disease and not when the fibrosis is already established (Pini *et al*., 2012). Therefore, options oriented towards new therapeutic targets and combined therapies which could override the limits of the existing anti-inflammatory drugs are urgently required. In particular, it could be possible to design combination-based approaches targeting events that are down-stream in the disease cascade compared with those that are up-stream, as fibroblast activation is crucial to the disease progression (Sivakumar *et al*., 2012).

In vitro studies have shown that histamine is able to stimulate foreskin fibroblast proliferation, collagen synthesis (Garbuzenko *et al*., 2002) and conjunctival fibroblast migration (Leonardi *et al*., 1999). The observation that histamine H_4 receptor (H_4R) is present in the bronchial epithelial, smooth muscle and micro-vascular endothelial cells of the lung (Gantner *et al*., 2002), suggests a possible involvement of this receptor in different airway diseases. More recently, Kohyama *et al.*, (2010) demonstrated, in human foetal lung fibroblasts, that JNJ7777120, a selective H_4R antagonist, prevents fibronectin-induced lung fibroblast migration, thus suggesting that H_4R could represent an attractive target for the development of new drugs for lung fibrosis treatment (Kohyama *et al*., 2010). In addition, H_4R antagonists were found to reduce collagen deposition and Goblet cell hyperplasia in a model of allergic asthma (Cowden *et al*., 2010). The aim of the present study was to validate the hypothesis that a combination-based strategy with an H_4R antagonist and a NSAID could be effective in pulmonary fibrosis. For this purpose we have evaluated the relative effect of the H_4R selective antagonist JNJ7777120, naproxen and their combination in the *in vivo* mouse model of bleomycin-induced lung fibrosis.

JPET Fast Forward. Published on September 2, 2014 as DOI: 10.1124/jpet.114.215152
This article has not been copyedited and formatted. The final version may differ from this version.

Methods

Animals. Fifty male C57BL/6 mice, about 2-months old and weighing 25-30 g were used for the experiments. They were purchased from a commercial dealer (Harlan, Udine, Italy) and housed in a controlled environment for 3 days at 22°C with a 12-h light/12-h dark cycle before use. During the experimental time the animals were maintained in the same conditions as reported above and provided with standard chow and water *at libitum.* The experimental protocols were designed in compliance with the Italian and the European Community regulations on animal experimentation for scientific purposes (D.M. 116192; O.J. of E.C. L358/1 12/18/1986) and in agreement with the Good Laboratory Practice. The protocols were approved by the Ethical Committee of the University of Florence, Italy. Experiments were carried out at the Centre for Laboratory Animal Housing and Experimentation (CeSAL), University of Florence, Italy.

Surgery and Treatments. The mice were anesthetized with zolazepam/tiletamine (Zoletil, Virbac Srl, Milan, Italy; 50 μg/g in 100 μl saline, i.p.); 40 were treated with bleomycin (0.05 IU in 100 μl saline) and other 10 with 100 μl saline (referred to as non-fibrotic negative controls), both delivered by tracheal injection. The bleomycin-treated mice were randomly assessed to receive, by subcutaneusly implanted micro-osmotic pump (ALZET Osmotic Pumps, Cupertino, CA, USA), vehicle alone (referred to as fibrotic positive controls), the 1-[(5-chloro-1H-indol-2-yl)carbonyl]-4-methylpiperazine, JNJ7777120 (Hill *et al.*, 1997) kindly provided by Johnson & Johnson Pharmaceutical and Development, San Diego, CA, USA (total dose 40 mg/kg b.wt.), the 2-(6-methoxynaphthalen-2-yl)propanoic acid, known as naproxen, (total dose 21 mg/kg b.wt.) or a combination of both for 15 days after surgery. The micro-osmotic pump allows the release of 0.11 μl/h of drug, for a daily dosage of 1.056 mg/kg for JNJ7777120 and of 0.55 mg/kg for naproxen. The dose of JNJ7777120 administered with the micro-osmotic pump was selected as the lower dose, which exerted an effect in a sub-chronic model of asthma (Cowden *et al*., 2010). Naproxen dose (0.55 mg/kg/die) was selected according to our previous results obtained in the same animal

model of fibrosis (Pini *et al.*, 2012) where 1mg/Kg already showed the maximal effect; in the present study we investigated the efficacy of the combination of the two compounds in order to reduce the toxicity of naproxen (ED_{50} 3.7 mg/kg).

Functional Assay of Fibrosis. At day 14 after surgery, the mice were subjected to measurement of airway resistance to inflation, a functional parameter related to fibrosis-induced lung stiffness, using a constant volume mechanical ventilation method (Masini *et al.*, 2005). Briefly, upon anesthesia, the mice were operated to insert a 22-gauge cannula (Venflon 2, 0.8 mm diameter) into the trachea and then ventilated with a small-animal respirator (Ugo Basile, Bologna, Italy), adjusted to deliver a tidal volume of 0.8 ml at a rate of 20 strokes/min. Changes in lung resistance to inflation (pressure at the airway opening, PAO) were registered by a high sensitivity pressure transducer (P75 type 379, HSE, Germany) connected to a polygraph (Harvard, UK; settings: gain 1, chart speed 25 mm/s). Inflation pressure was measured for at least 3 min. In each mouse, PAO measurements (expressed as mm on the chart) were carried out on at least 40 consecutive tracings of respiratory strokes after breathing stabilization and then averaged.

Lung Tissue Sampling. After the functional assay, the animals were killed with lethal dose of anesthetic drugs and the whole left lungs were excised and fixed by immersion in 4% formaldehyde in PBS for histological analysis. The right lungs were weighed, quickly frozen and stored at -80° C. When needed for the biochemical assays, these samples were thawed at 4° C, homogenized on ice in 50 mM Tris-HCl buffer containing 180 mM KCl and 10 mM EDTA, final pH 7.4, and then centrifuged at 10,000 *g*, 4° C, for 30 min, unless otherwise reported. The supernatants and the pellets were collected and used for separate assays, as detailed below.

Histology and Computer-Aided Densitometry of Lung Collagen. Histological sections, 6 μm thick, were cut from paraffin-embedded lung samples and stained with hematoxylin and eosin for

routine observation, periodic acid-Schiff (PAS) or modified Azan method (Pini *et al*., 2010) for the evaluation of goblet cells and collagen deposition. Staining was performed in a single session, to minimize the artifactual differences in collagen staining. For each mouse, 20 photomicrographs of peri-bronchial connective tissue were randomly taken using a digital camera connected to a light microscope with a 40x objective (test area of each micrograph: 38,700 μm^2). Measurements of optical density (OD) of the aniline blue-stained collagen fibers were carried out using ImageJ 1.33 image analysis program (http://rsb.info.nih.gov/ij), upon appropriate threshold selection to exclude aerial air spaces and bronchial/alveolar epithelium, as previously described (Pini *et al*., 2010). For morphometry of smooth muscle layer thickness and bronchial goblet cell numbers, both key markers of airway remodeling, lung tissue sections were stained with hematoxylin and eosin or with PAS staining for mucins, respectively. Digital photomicrographs of medium- and small-sized bronchi were randomly taken. Measurements of the thickness of the bronchial smooth muscle layer were carried out on the digitized images using the above-mentioned software. PAS-stained goblet cells and total bronchial epithelial cells were counted on bronchial cross-section profiles, and the percentage of goblet cells was calculated. For all these parameters, values are means ± S.E.M. of individual mice (twenty images each) from the different experimental groups.

Determination of Transforming Growth Factor (TGF)-β Levels. The levels of TGF-β, the major pro-fibrotic cytokine involved in fibroblast activation (Wynn, 2008), were measured on aliquots (100 μl) of lung homogenate supernatants using the Flow Cytomix assay (Bender Medsystems GmbH, Vienna, Austria), following the protocol provided by the manufacturer. Briefly, a suspension of anti-TGF-β-coated beads was incubated with the samples (and a TGF-β standard curve) and then with biotin-conjugated secondary antibodies and streptavidin-phycoerythrin. Fluorescence was read with a cytofluorimeter (Epics XL, Beckman Coulter, Milan, Italy). Values are expressed as pg/mg proteins, the latter determined with the Bradford method (Bradford, 1976) over an albumin standard curve.

Determination of Myeloperoxidase (MPO) Activity. This tissue indicator of leukocyte recruitment was determined as described by the literature (Mullane *et al*., 1985). Briefly, frozen lung tissue samples of about 50-70 mg were homogenized in a solution containing 0.5% hexadodecyltrimethyl-ammonium bromide dissolved in 10 mmol/L potassium phosphate buffer, pH 7 and then centrifuged for 30 min at 20,000 g at 4° C. An aliquot of the supernatant was then allowed to react with a solution of tetra-methyl-benzidine (1.6 mmol/L) and 0.1 mmol/L H_2O_2. The rate of change in absorbance was measured spectrophotometrically at 650 nm. Myeloperoxidase activity was defined as the quantity of enzyme degrading 1 μmol of peroxide per min at 37°C and was expressed in mU/mg of proteins, determined with the Bradford method (Bradford, 1976) over an albumin standard curve

Determination of Prostaglandin E_2 (PGE_2) and Interleukin $(IL)_{10}$ levels. The levels of PGE_2, the major cyclooxygenase product generated by activated inflammatory cells, and the levels of IL_{10}, a well-known anti-inflammatory cytokine, were measured on aliquots (100 μl) of lung homogenate supernatants using a commercial ELISA Biotrak™ kits (Amesham Biosciences, U.K.) following the protocol provided by the manufacturer. The values are expressed as ng/mg of proteins, the latter determined with the Bradford method (Bradford, 1976) over an albumin standard curve.

Determination of Oxidative Stress Parameters. Malonyldialdehyde (MDA) is an end-product of peroxidation of cell membrane lipids caused by oxygen-derived free radicals and is considered a reliable marker of inflammatory tissue damage. It was determined as thiobarbituric acid-reactive substance (TBARS) levels as described previously (Ohkawa *et al*., 1979). Approximately 100 mg of lung tissue were homogenized with 1 ml of 50 mmol/L Tris-HCl buffer containing 180 mmol/L KCl and 10 mmol/L EDTA, final pH 7.4. 0.5 ml of 2-thiobarbituric acid (1% w/v) in 0.05 mol/L NaOH and 0.5 ml of HCl (25% w/v in water) were added to 0.5 ml of sample. The mixture was

placed in test tubes, sealed with screw caps, and heated in boiling water for 10 min. After cooling, the chromogen was extracted in 3 ml of 1-butanol, and the organic phase was separated by centrifugation at 2,000 x g for 10 min. The absorbance of the organic phase was read spectrophotometrically at 532 nm wave length. The values are expressed as nmol of TBARS (MDA equivalents)/mg of protein, using a standard curve of 1,1,3,3-tetramethoxypropane.

As indicator of oxidative DNA damage the levels of 8-hydroxy-2'-deoxyguanosine (8-OH*d*G) were determined as previously described (Lodovici *et al.*, 2000). Briefly, lung samples were homogenized in 1ml of 10 mM PBS, pH 7.4, sonicated on ice for 1 min, added with 1 ml of 10 mmol/L Tris-HCl buffer, pH 8, containing 10 mmol/L EDTA, 10 mmol/L NaCl, and 0.5% SDS, incubated for 1 h at 37°C with 20 μg/ml RNase 1 (Sigma-Aldrich) and overnight at 37°C under argon in the presence of 100 μg/ml proteinase K (Sigma-Aldrich). The mixture was extracted with chloroform/isoamyl alcohol (10/2 v/v). DNA was precipitated from the aqueous phase with 0.2 volumes of 10 mmol/L ammonium acetate, solubilized in 200 μl of 20 mmol/L acetate buffer, pH 5.3, and denatured at 90°C for 3 min. The extract was then supplemented with 10 IU of P1 nuclease (Sigma-Aldrich) in 10 μl and incubated for 1 h at 37°C with 5 IU of alkaline phosphatase (Sigma-Aldrich) in 0.4 mol/L phosphate buffer, pH 8.8. All of the procedures were performed in the dark under argon. The mixture was filtered by an Amicon Micropure-EZ filter (Millipore Corporation, Billerica, MA), and 50 μl of each sample was used for 8-OH*d*G determination using a Bioxytech enzyme immunoassay kit (Oxis, Portland, OR), following the instructions provided by the manufacturer. The values are expressed as ng 8-OH*d*G/mg of proteins, the latter determined with the Bradford method (Bradford, 1976) over an albumin standard curve.

Determination of Smad3 Level expression. Tissue samples were homogenized on ice and lysed as previously reported (Sassoli *et al.*, 2012). One mg of total protein extract was pre-cleared by Protein G (Sigma-Aldrich, St Louis, MO, USA) for 1 h at 4°C. After centrifugation, the supernatants were collected and incubated overnight at 4°C with 4 μg of goat polyclonal anti-Smad4 antibody (Santa

JPET Fast Forward. Published on September 2, 2014 as DOI: 10.1124/jpet.114.215152
This article has not been copyedited and formatted. The final version may differ from this version.

Cruz Biotechnologies, Santa Cruz, CA, USA). The immunocomplexes were recovered using Protein G, subjected to electrophoresis, blotted with rabbit polyclonal anti-Smad3 (1:1000 in T-TBS; Cell-Signaling Technology, Danvers, MA, USA) and then re-probed with anti-Smad4 antibody (1:1000 in T-TBS).

Statistical Analysis. For each assay, data were reported as mean values (± S.E.M) of individual average measures of the different animals per group. Significance of differences among the groups was assessed by one-way ANOVA followed by Newman-Keuls post-hoc test for multiple comparisons, using Graph Pad Prism 4.03 statistical software (GraphPad Software, INC., San Diego, CA, USA).

Results

Functional Assay of Fibrosis. Intratracheal bleomycin caused a statistically significant increase in airway stiffness as judged by the significant elevation of PAO (Fig.1) in the fibrotic positive controls compared with the non-fibrotic negative ones (+2.06 ± 0.25 mm; $P<0.001$). Both naproxen and JNJ7777120 given alone caused a significant reduction of bleomycin-induced airway stiffness. The efficacy of JNJ7777120 seemed slightly higher than that of equimolar naproxene (-1.30 ± 0.21 mm and -1.07 ± 0.22 mm for JNJ7777120 and naproxen, respectively), although the differences did not reach statistical significance. Similar results were obtained when the two drugs were co-administrated.

Morphological and morphometrical analyses. Intratracheal bleomycin administration was found to cause lung inflammation and fibrosis. By computer-aided densitometry on Azan-stained sections (Fig. 2), which allows the determination of the OD of collagen fibers, the lungs of the fibrotic positive controls demonstrated an increase in collagen fibers, that was significantly reduced by both JNJ7777120 and naproxen given alone ($P<0.01$, and $P<0.05$, respectively). When the two drugs were given together a trend towards an increased effect was observed. The extent of the inflammatory infiltrate, which was composed mainly of macrophages, lymphocytes and neutrophils, was reduced by all the treatments. We then evaluated bronchial remodelling by measuring the relative number of goblet cells (Fig. 3) and the thickness of the smooth muscle (Fig. 4), key histological parameters of inflammation-induced adverse bronchial remodelling (Bai and Knight, 2005). As expected, both these parameters were significantly increased after intratracheal bleomycin treatment (+10.09 ± 1.30 %, $P<0.001$ for goblet cells number and +27.38 ± 3.35 μm, $P<0.001$ for thickness of the smooth muscle). JNJ7777120 and naproxen both alone or in combination were able to significantly reduce the percentage of PAS-positive goblet cells over total bronchial epithelial cells (-7.83 ± 1.21 %, $P<0.05$ and -5.74 ± 1.38 %, $P<0.05$, respectively), as well as the thickness of the airway smooth muscle layer (-22.40 ± 3.03 μm, $P<0.01$ and -18.97 ± 3.50

μm, $P<0.05$, respectively). Notably, the combination of the two drugs showed a statistically significant reduction of the fraction of goblet cells compared to the treatment with naproxen alone (-4.46 ± 1.38 %; $P<0.05$).

Determination of inflammation and fibrosis parameters. Assay of TGF-β (Fig. 5A), a major pro-fibrotic cytokine, showed that this molecule significantly increased in the fibrotic positive controls (+274.9 ± 13.68 pg/mg protein; $P<0.001$). JNJ7777120 or naproxen treatment caused a statistically significant and comparable reduction of TGF-β (-116.2 ± 6.98 pg/mg protein and -123.0 ± 6.84 pg/mg protein, respectively; $P<0.01$ for both). Notably, the co-administration of both drugs was more effective than JNJ7777120 or naproxen alone (-93.83 ± 6.68 pg/mg protein *vs.* JNJ7777120 and -87.12 ± 5.60 pg/mg protein *vs.* naproxen; $P<0.01$). As the Smad3/4 complex is necessary for activation of TGF-β signaling (Chen *et al*., 2005), we investigated the effect of the pharmacological treatment on the complex formation by Western blotting analysis performed on the immunoprecipitated Smad4 protein. As shown in Fig. 5B, just above the heavy chain of IgG, we identify a 61 kDa protein band consistent with Smad4. Notably, when we blotted with the anti-Smad3 antibody, we observed a profound up-regulation in the positive fibrotic control that was prevented by JNJ7777120 and naproxen given alone. Intriguingly, as shown for TGF-β levels, the co-administration of the two drugs was more effective.

Determination of MPO (Fig. 6A), an index of leukocyte accumulation into the inflamed lung tissue, showed that this parameter was significantly increased in the fibrotic positive controls compared with non-fibrotic negative ones. Administration of JNJ7777120 or naproxen caused a statistically significant reduction of MPO induced by bleomycin (-9.53 ± 0.28, -9.39 ± 0.027 mU/mg protein for JNJ7777120 and naproxen, respectively; $P<0.001$). When the two drugs were co-administrated an increased effect was observed (-11.27 ± 0.34; $P<0.05$).

Determination of PGE_2 (Fig. 6B), the major cyclooxygenase product generated by activated inflammatory cells, fibroblasts included, showed that this mediator was markedly increased in the

JPET Fast Forward. Published on September 2, 2014 as DOI: 10.1124/jpet.114.215152
This article has not been copyedited and formatted. The final version may differ from this version.

fibrotic positive controls when compared with the non-fibrotic negative controls (+52.08 ± 2.69 pg/mg protein; $P<0.001$). JNJ7777120 or naproxen given alone caused a statistically significant reduction of PGE_2 level, with naproxen, as expected, more effective than JNJ7777120 (-16.20 ± 2.36 pg/mg protein for JNJ7777120 and -35.30 ± 2.36 pg/mg protein for naproxen; $P<0.01$). However, the combination of the two drugs was more effective in reducing PGE_2 production in comparison to the single drugs (-28.26 ± 2.23 pg/mg protein *vs* JNJ7777120, $P<0.01$; and -9.16 ± 2.23 pg/mg protein *vs* naproxen $P<0.001$). To confirm the anti-inflammatory effects of the two studied drugs we evaluated IL_{10} production, a regulatory cytokine (Fig. 6C). As expected, bleomycin-treated animals showed a significant reduction in IL_{10} levels (-17.05 ± 1.51, $P<0.001$) whereas the administration of both JNJ7777120 or naproxen alone or in combination caused a statistically significant increased of IL_{10} levels ($P<0.01$). When the two drugs were co-administrated a potentiated effect was observed.

Evaluation of oxidative stress parameters. Measurement of TBARS (Fig. 7A), a reliable marker of oxidative tissue injury being the end products of cell membrane lipid peroxidation by ROS, and of 8-OH*d*G (Fig. 7B), an indicator of oxidative DNA damage, showed that they were markedly increased in fibrotic positive controls (+41.33 ± 11.15 nmol/mg protein and +51.25 ± 2.77 ng/mg protein, respectively; $P<0.001$) compared with non-fibrotic negative control; these parameters were significantly reduced by JNJ7777120 (-18.17 ± 5.66 nmol/mg protein, -33.46 ± 2.65 ng/mg protein, respectively; $P<0.01$) or naproxen (-23.50 ± 7.32 nmol/mg protein, -33.48 ± 2.65 ng/mg protein, respectively; $P<0.01$). Notably, the combination of JNJ7777120 and naproxen was more effective in reducing MDA levels than JNJ7777120 (-14.08 ± 4.8 nmol/mg protein; $P<0.05$) or naproxen (-8.74 ± 2.98 nmol/mg protein; $P<0.01$) treatment alone. A slight but not significant effect was also observed also in 8-OH*d*G production.

Discussion

The data presented in this work demonstrate the anti-inflammatory and anti-fibrotic properties of naproxen and JNJ7777120 in a mouse model of lung fibrosis. We selected the model of bleomycin, intra-tracheally delivered, because it is the best characterized murine model in use today for lung fibrosis. Intratracheal delivery of bleomicyn to rodents results in a direct damage initially to alveolar epithelial cells, followed by the development of neutrophilic and lymphocytic pan-alveolitis within the first week and the development of fibrosis by day 14, with maximal responses generally around days 21–28 (Moore and Hogaboam, 2008). Chronic inflammatory conditions in the lungs lead to permanent structural changes and remodeling of the airway walls, whose fibrosis is a major constituent. Nowadays, there are no approved drugs that counteract the pathological mechanism apart for some potential treatments targeting TGF-β1 pathway, e.g. pirfenidone (Paz and Shoenfeld, 2010). Our experiments were performed in C57BL/6 mice, which are reported to be more susceptible to bleomycin-induced fibrosis than other strains, such as Balb/c mice (Schrier *et al.*, 1983; Harrison and Lazo, 1987). Both drugs given alone or in combination were administered after the onset of bleomycin-induced lung injury, by using a subcutaneously implanted micro-osmotic pump. This system allows sustained and long-term drug delivery, thus overcoming the pharmacokinetic limits of JNJ7777120, which has a maximal oral bioavailability of about 30% and a terminal half-life in mice of 1 h (Thurmond *et al.*, 2004).

In our experimental model JNJ7777120, a selective receptor antagonist for H_4R has been compared with equimolar doses of naproxen. Compound JNJ7777120 has shown strong anti-inflammatory properties, significantly decreasing the histological and biochemical inflammatory parameters, such as the number of infiltrating leukocytes, PGE_2 and IL_{10} levels. When looking at the reduction of PGE_2 levels, which solely depend on COX inhibition, naproxen had a higher efficacy than JNJ7777120 ($p<0.001$). On the other hand, when considering the other parameters, such as inhibition of leukocyte infiltration in the lung tissue and oxidative stress markers, JNJ7777120 was a little more effective than naproxen. When the two drugs were given together we

JPET Fast Forward. Published on September 2, 2014 as DOI: 10.1124/jpet.114.215152
This article has not been copyedited and formatted. The final version may differ from this version.

observed an additional effect conceivably determined by the complementary mechanisms acting on different pro-inflammatory targets. However, it can be speculated that anti-TGF-β activity of JNJ7777120 may indirectly affects eicosanoid pathways, by reducing TGF-β/Smad signaling which is known to induce COX-2. Moreover, the hypothesis of a link between PGE_2 and TGF-β, already suggested (Alfranca *et al*., 2008), is herein supported; indeed, also naproxen down-regulates TGF-β levels and Smad3/4 complex formation. COX-1 and COX-2 inhibitors, such as indomethacin, diclofenac, meloxican and naproxen were reported to reduce lung collagen accumulation, inflammation and oxidative stress in bleomicyn-induced lung fibrosis model (Thrall *et al.*, 1979; Chandler and Young, 1989; Arafa *et al.*, 2007; Pini *et al.*, 2012), a model that highlights the inflammatory component of the pathology. Indeed high levels of PGE_2 were reported in our positive fibrotic controls. However, evidence exist that PGE_2 has anti-inflammatory effects and inhibits collagen production (Saltzman *et al*., 1982) and that PGE_2 levels in patients with pulmonary fibrosis are significantly decreased, suggesting an ambiguous role of PGE_2 in lung fibroblast homeostasis. It is possible that prostaglandin inhibition can have a positive effect on the onset of lung fibrosis during the initial phase of inflammation and a detrimental effect during the fibrogenic events.

On the other side, the available data strongly support the H_4R as a novel target for the pharmacological modulation of immune and inflammatory disorders (Masini *et al.*, 2013). Indeed, in inflammatory lung disorders, histamine acts as a mediator of both acute and chronic phases. The H_4R are present in low amounts in the lung, where its expression in bronchial epithelial and smooth muscle cells and micro-vascular endothelial cells (Gantner *et al.*, 2002) can differently contribute to airway diseases. H_4R mediates redistribution and recruitment of mast cells in mucosal epithelium after allergen exposure (Thurmond *et al.*, 2004), mediates the synergistic action of histamine and CXCL12, a chemokine involved in airway allergic disorders (Godot *et al*., 2007) and mediates the recruitment and response of Treg cells (Morgan *et al.*, 2007).

The relevant effects of JNJ7777120 could be explained through the marked decrease on leukocyte infiltration in this *in vivo* model of pulmonary fibrosis, thus adding further evidence to the

JPET Fast Forward. Published on September 2, 2014 as DOI: 10.1124/jpet.114.215152
This article has not been copyedited and formatted. The final version may differ from this version.

role of this receptor in controlling leukocyte trafficking and pro-inflammatory responses (Zampeli and Tiligada, 2009). These data suggest that JNJ7777120 may exert not only a favorable effect during the overt inflammatory phase of the disease, as previously reported with naproxen (Pini *et al*., 2012), but also during fibroblast proliferation. Indeed, previous data demonstrated a role for histamine and H_4R in fibroblast activation (Cowden *et al.*, 2010), which is a pivotal event in the pathological process related to the disease progression (Garbuzenko *et al.*, 2002; Kohyama *et al.*, 2010). Here we report the effects of JNJ7777120 on the lung TGF-β pathway, collagen deposition and goblet cell hyperplasia. In keeping with the demonstration that histamine modulates TGF-β/Smad signaling in conjunctival fibroblasts (Leonardi *et al*., 2010), our data confirm that the pro-fibrotic effect of histamine is regulated by the activation of H_4R. Taken together these results clearly indicate the anti-fibrotic effect of the H_4R antagonist.

On this background, our study points at the association between the two drugs as a promising therapeutic approach for pulmonary fibrosis. When naproxen and JNJ7777120 were co-administrated, additive positive effects were measured on lung TGF-β signalling modulation, PGE_2, leukocytes and goblet cell infiltration, confirming the effects of these drugs on the inflammatory phase. A single time point (24 days) was planned for this study. At this time-point a maximal fibrotic response was observed and JNJ7777120 and naproxen, given in combination, exerted a maximal effect on most of the studied parameters.

Our data suggest that Smad3/4 complex formation plays a major role in determining the pharmacological efficacy of the combination strategy herein proposed. Indeed, we propose that JNJ7777120, reducing TGF-β and Smad3/4 complex formation, contributes to PGE_2 reduction, which is further affected by naproxen, inhibiting COX-2. Therefore, by abolishing the PGE_2-mediated positive feed-back on TGF-β/Smad signaling this strategy results more effective than the each drug alone.

JPET Fast Forward. Published on September 2, 2014 as DOI: 10.1124/jpet.114.215152
This article has not been copyedited and formatted. The final version may differ from this version.

In conclusion, the results of the present study, supporting the hypothesis that H_4R antagonism exerts anti-inflammatory and anti-fibrotic effects in the model of bleomycin-induced lung fibrosis, indicate the therapeutic potential of the combination of H_4R antagonists and NSAIDs. Although JNJ7777120 itself is emerging as a promising therapeutic agent in lung inflammation and fibrosis, the association with naproxen can have a distinct advantage over the single drug for the potentiating effect on the inhibition of inflammatory and pro-fibrotic parameters. Moreover, this strategy could override the safety limitations of the existing anti-inflammatory drugs in the treatment of pulmonary fibrosis.

JPET Fast Forward. Published on September 2, 2014 as DOI: 10.1124/jpet.114.215152
This article has not been copyedited and formatted. The final version may differ from this version.

Authorship contributions

Participated in research design: A.C.R., H.S., R.L.T., E.M.

Conducted experiments: A.C.R., A.P., L.L., E.V.,C.L.

Performed data analysis : A.P.

Wrote or contributed to the writing of the manuscript: A.C.R., E.V., E.M.

References

Alfranca A, Lopez-Oliva JM, Genis L, Lopez-Maderuelo D, Mirones I, Salvado D, Quesada AJ, Arroyo AG and Redondo JM (2008) PGE2 induces angiogenesis via MT1-MMP-mediated activation of the TGFbeta/Alk5 signaling pathway. *Blood* **112**:1120-1128.

Arafa HM, Abdel-Wahab MH, El-Shafeey MF, Badary OA and Hamada FM (2007) Anti-fibrotic effect of meloxicam in a murine lung fibrosis model. *Eur J Pharmacol* **564**:181-189.

Bai TR and Knight DA (2005) Structural changes in the airways in asthma: observations and consequences. *Clin Sci (Lond)* **108**:463-477.

Bradford MM (1976) A rapid and sensitive method for the quantitation of microgram quantities of protein utilizing the principle of protein-dye binding. *Anal Biochem* **72**:248-254.

Carter NJ (2011) Pirfenidone: in idiopathic pulmonary fibrosis. *Drugs* **71**:1721-1732.

Chandler DB and Young K (1989) The effect of diclofenac acid (Voltaren) on bleomycin-induced pulmonary fibrosis in hamsters. *Prostaglandins Leukot Essent Fatty Acids* **38**:9-14.

Chen HB, Rud JG, Lin K and Xu L (2005) Nuclear targeting of transforming growth factor-beta-activated Smad complexes. *J Biol Chem* **280**:21329-21336.

Cowden JM, Riley JP, Ma JY, Thurmond RL and Dunford PJ (2010) Histamine H4 receptor antagonism diminishes existing airway inflammation and dysfunction via modulation of Th2 cytokines. *Respir Res* **11**:86.

Davies HR, Richeldi L and Walters EH (2003) Immunomodulatory agents for idiopathic pulmonary fibrosis. *Cochrane Database Syst Rev*:CD003134.

du Bois RM (2010) Strategies for treating idiopathic pulmonary fibrosis. *Nat Rev Drug Discov* **9**:129-140.

Gantner F, Sakai K, Tusche MW, Cruikshank WW, Center DM and Bacon KB (2002) Histamine h(4) and h(2) receptors control histamine-induced interleukin-16 release from human CD8(+) T cells. *J Pharmacol Exp Ther* **303**:300-307.

Garbuzenko E, Nagler A, Pickholtz D, Gillery P, Reich R, Maquart FX and Levi-Schaffer F (2002) Human mast cells stimulate fibroblast proliferation, collagen synthesis and lattice contraction: a direct role for mast cells in skin fibrosis. *Clin Exp Allergy* **32**:237-246.

Godot V, Arock M, Garcia G, Capel F, Flys C, Dy M, Emilie D and Humbert M (2007) H4 histamine receptor mediates optimal migration of mast cell precursors to CXCL12. *J Allergy Clin Immunol* **120**:827-834.

Harrison JH, Jr. and Lazo JS (1987) High dose continuous infusion of bleomycin in mice: a new model for drug-induced pulmonary fibrosis. *J Pharmacol Exp Ther* **243**:1185-1194.

Hauber HP and Blaukovitsch M (2010) Current and future treatment options in idiopathic pulmonary fibrosis. *Inflamm Allergy Drug Targets* **9**:158-172.

Kohyama T, Yamauchi Y, Takizawa H, Kamitani S, Kawasaki S and Nagase T (2010) Histamine stimulates human lung fibroblast migration. *Mol Cell Biochem* **337**:77-81.

Leonardi A, Di Stefano A, Motterle L, Zavan B, Abatangelo G and Brun P (2010) Transforming growth factor-beta/Smad - signalling pathway and conjunctival remodelling in vernal keratoconjunctivitis. *Clin Exp Allergy* **41**:52-60.

Leonardi A, Radice M, Fregona IA, Plebani M, Abatangelo G and Secchi AG (1999) Histamine effects on conjunctival fibroblasts from patients with vernal conjunctivitis. *Exp Eye Res* **68**:739-746.

Lodovici M, Casalini C, Cariaggi R, Michelucci L and Dolara P (2000) Levels of 8-hydroxydeoxyguanosine as a marker of DNA damage in human leukocytes. *Free Radic Biol Med* **28**:13-17.

Masini E, Bani D, Vannacci A, Pierpaoli S, Mannaioni PF, Comhair SA, Xu W, Muscoli C, Erzurum SC and Salvemini D (2005) Reduction of antigen-induced respiratory abnormalities and airway inflammation in sensitized guinea pigs by a superoxide dismutase mimetic. *Free Radic Biol Med* **39**:520-531.

Masini E, Lucarini L, Sydbom A, Dahlén B and Dahlén S-E (2013) Histamine in asthmatic and fibrotic disorders, in *Histamine H4 receptor: A novel drug target* (Stark H ed) pp 145-171, Versita, London.

Moore BB and Hogaboam CM (2008) Murine models of pulmonary fibrosis. *Am J Physiol Lung Cell Mol Physiol* **294**:L152-160.

Morgan RK, McAllister B, Cross L, Green DS, Kornfeld H, Center DM and Cruikshank WW (2007) Histamine 4 receptor activation induces recruitment of FoxP3+ T cells and inhibits allergic asthma in a murine model. *J Immunol* **178**:8081-8089.

Mullane KM, Kraemer R and Smith B (1985) Myeloperoxidase activity as a quantitative assessment of neutrophil infiltration into ischemic myocardium. *J Pharmacol Methods* **14**:157-167.

Ohkawa H, Ohishi N and Yagi K (1979) Assay for lipid peroxides in animal tissues by thiobarbituric acid reaction. *Anal Biochem* **95**:351-358.

Paz Z and Shoenfeld Y (2010) Antifibrosis: to reverse the irreversible. *Clin Rev Allergy Immunol* **38**:276-286.

Pini A, Shemesh R, Samuel CS, Bathgate RA, Zauberman A, Hermesh C, Wool A, Bani D and Rotman G (2010) Prevention of bleomycin-induced pulmonary fibrosis by a novel antifibrotic peptide with relaxin-like activity. *J Pharmacol Exp Ther* **335**:589-599.

Pini A, Viappiani S, Bolla M, Masini E and Bani D (2012) Prevention of bleomycin-induced lung fibrosis in mice by a novel approach of parallel inhibition of cyclooxygenase and nitric-oxide donation using NCX 466, a prototype cyclooxygenase inhibitor and nitric-oxide donor. *J Pharmacol Exp Ther* **341**:493-499.

Raghu G, Collard HR, Egan JJ, Martinez FJ, Behr J, Brown KK, Colby TV, Cordier JF, Flaherty KR, Lasky JA, Lynch DA, Ryu JH, Swigris JJ, Wells AU, Ancochea J, Bouros D, Carvalho C, Costabel U, Ebina M, Hansell DM, Johkoh T, Kim DS, King TE, Jr., Kondoh Y, Myers J, Muller NL, Nicholson AG, Richeldi L, Selman M, Dudden RF, Griss BS, Protzko SL and Schunemann HJ (2011) An official ATS/ERS/JRS/ALAT statement: idiopathic pulmonary

fibrosis: evidence-based guidelines for diagnosis and management. *Am J Respir Crit Care Med* **183**:788-824.

Richeldi L, Davies HR, Ferrara G and Franco F (2003) Corticosteroids for idiopathic pulmonary fibrosis. *Cochrane Database Syst Rev*:CD002880.

Saltzman LE, Moss J, Berg RA, Hom B and Crystal RG (1982) Modulation of collagen production by fibroblasts. Effects of chronic exposure to agonists that increase intracellular cyclic AMP. *Biochem J* **204**:25-30.

Sassoli C, Pini A, Chellini F, Mazzanti B, Nistri S, Nosi D, Saccardi R, Quercioli F, Zecchi-Orlandini S and Formigli L (2012) Bone marrow mesenchymal stromal cells stimulate skeletal myoblast proliferation through the paracrine release of VEGF. *PLoS One* **7**:e37512.

Schrier DJ, Kunkel RG and Phan SH (1983) The role of strain variation in murine bleomycin-induced pulmonary fibrosis. *Am Rev Respir Dis* **127**:63-66.

Sivakumar P, Ntolios P, Jenkins G and Laurent G (2012) Into the matrix: targeting fibroblasts in pulmonary fibrosis. *Curr Opin Pulm Med* **18**:462-469.

Stramer BM, Mori R and Martin P (2007) The inflammation-fibrosis link? A Jekyll and Hyde role for blood cells during wound repair. *J Invest Dermatol* **127**:1009-1017.

Thrall RS, McCormick JR, Jack RM, McReynolds RA and Ward PA (1979) Bleomycin-induced pulmonary fibrosis in the rat: inhibition by indomethacin. *Am J Pathol* **95**:117-130.

Thurmond RL, Desai PJ, Dunford PJ, Fung-Leung WP, Hofstra CL, Jiang W, Nguyen S, Riley JP, Sun S, Williams KN, Edwards JP and Karlsson L (2004) A potent and selective histamine H4 receptor antagonist with anti-inflammatory properties. *J Pharmacol Exp Ther* **309**:404-413.

Wynn TA (2008) Cellular and molecular mechanisms of fibrosis. *J Pathol* **214**:199-210.

Zampeli E and Tiligada E (2009) The role of histamine H4 receptor in immune and inflammatory disorders. *Br J Pharmacol* **157**:24-33.

Footnotes

This work was supported by COST Action BM0806 (A.C.R., A.P.; H.S. and E.M.) and from Ente Cassa di Risparmio di Firenze, Florence, Italy (E.M.). Part of this study was presented at the 40th EHRS meeting, 11-14th May 2011 Sochi, Russia and published in abstract form in *Inflamm. Res.* Sep 2011; 60(2): S335-S335.

Legends for Figures

Fig. 1. Spirometric evaluation. Bar graph and statistical analysis of differences of pressure at the airway opening (PAO) values (means± S.E.M) between the different experimental groups (one way ANOVA; n=10 animals per group). ***P*<0.01 and ****P*<0.001 *vs*. bleomycin + vehicle.

Fig. 2. Evaluation of lung fibrosis. Panel A: representative micrographs of Azan-stained lung tissue sections from mice of the different experimental groups. Collagen fibers are deep blue stained. The lung from fibrotic control treated with vehicle showed marked fibrosis in the peri-bronchial stroma, which was absent in the lung from non-fibrotic negative control and reduced by both JNJ7777120 and naproxen either alone or in combination. Panel B: bar graph showing the optical density (OD, means± S.E.M.) of Azan-stained collagen fibers of the different experimental groups (one way ANOVA, n=10 mice per group). **P*<0.05, ***P*<0.01 and ****P*<0.001 *vs*. bleomycin + vehicle.

Fig. 3 Goblet cell hyperplasia. Panel A: Representative micrographs of PAS-stained sections. Arrows indicate the goblet cells. Panel B: bar graph showing the fraction of goblet cells (% means ± S.E.M.) in the different experimental groups (one way ANOVA, n=10 animals per group). **P*<0.05, ***P*<0.01 and ****P*<0.001 *vs*. bleomycin + vehicle; # *P*<0.05 *vs*. bleomycin + naproxen.

Fig. 4. Evaluation of the muscular remodeling. The smooth muscle thickness was assessed by computer-aided morphometry on hematoxylin and eosin-stained lung sections. Panel A: representative micrographs of the sections. The thickness of the smooth muscle layer is indicated by double arrows. Panel B: bar graph showing the length (μm) of the muscular fiber (means ± S.E.M.) in the different experimental groups (one way ANOVA, n=10 animal per group). **P*<0.05, ***P*<0.01*vs*. bleomycin+vehicle.

JPET Fast Forward. Published on September 2, 2014 as DOI: 10.1124/jpet.114.215152
This article has not been copyedited and formatted. The final version may differ from this version.

Fig. 5. Evaluation of fibrotic key mediators. Panel A: Bar graph showing the lung tissue levels of the pro-fibrotic cytokine TGF-β (means ± S.E.M.) of the different experimental groups (one way ANOVA, n=10 animals per group). Panel B: Smad4 and Smad3 expression level in the noted experimental conditions, assayed by Western Blotting analysis performed on the immunoprecipitated Smad4 protein. Note that the profound up-regulation of Smad3 expression level in the positive fibrotic control was prevented by the treatment with both JNJ7777120 or naproxen alone. The co-administration of the two drugs was more effective. ***P*<0.01 and ****P*<0.001 *vs.* bleomycin + vehicle; °°*P*<0.01 *vs.* bleomycin+JNJ7777120; ##*P*<0.01 *vs*. bleomycin + naproxen.

Fig. 6. Evaluation inflammation parameters. Panel A: bar graph showing the tissue level (means ± S.E.M.) of the enzyme MPO, evaluated as the quantity of enzyme degrading 1 μmol of peroxide/min at 37 °C, of the different experimental groups. Panel B: bar graph showing the tissue levels of the PGE_2 (means ± S.E.M.) of the different experimental groups. Panel C. Bar graph showing the tissue levels of the anti-inflammatory cytokine IL_{10} (means ± S.E.M.) of the different experimental groups (one way ANOVA, n=10 animals per group). ***P*<0.01 and ****P*<0.001 *vs.* bleomycin + vehicle; °*P*<0.05 and °°*P*<0.01 *vs*. bleomycin+JNJ7777120; # *P*<0.05 and ###*P*<0.001 *vs*. bleomycin + naproxen.

Fig. 7. Evaluation of oxidative stress parameters. Panel A: bar graph showing the lung tissue of TBARS (means ± S.E.M.) in the different experimental groups. Panel B: bar graph showing the levels of 8-OH*d*G (means ± S.E.M.) in the different experimental groups (one way ANOVA, n=10 animals/group). °*P*<0.05 *vs.* bleomycin + JNJ7777120; ##*P*<0.01 *vs.* bleomycin+naproxen; ***P*<0.01 and ****P*<0.001 *vs.* bleomycin + vehicle.

Fig. 1

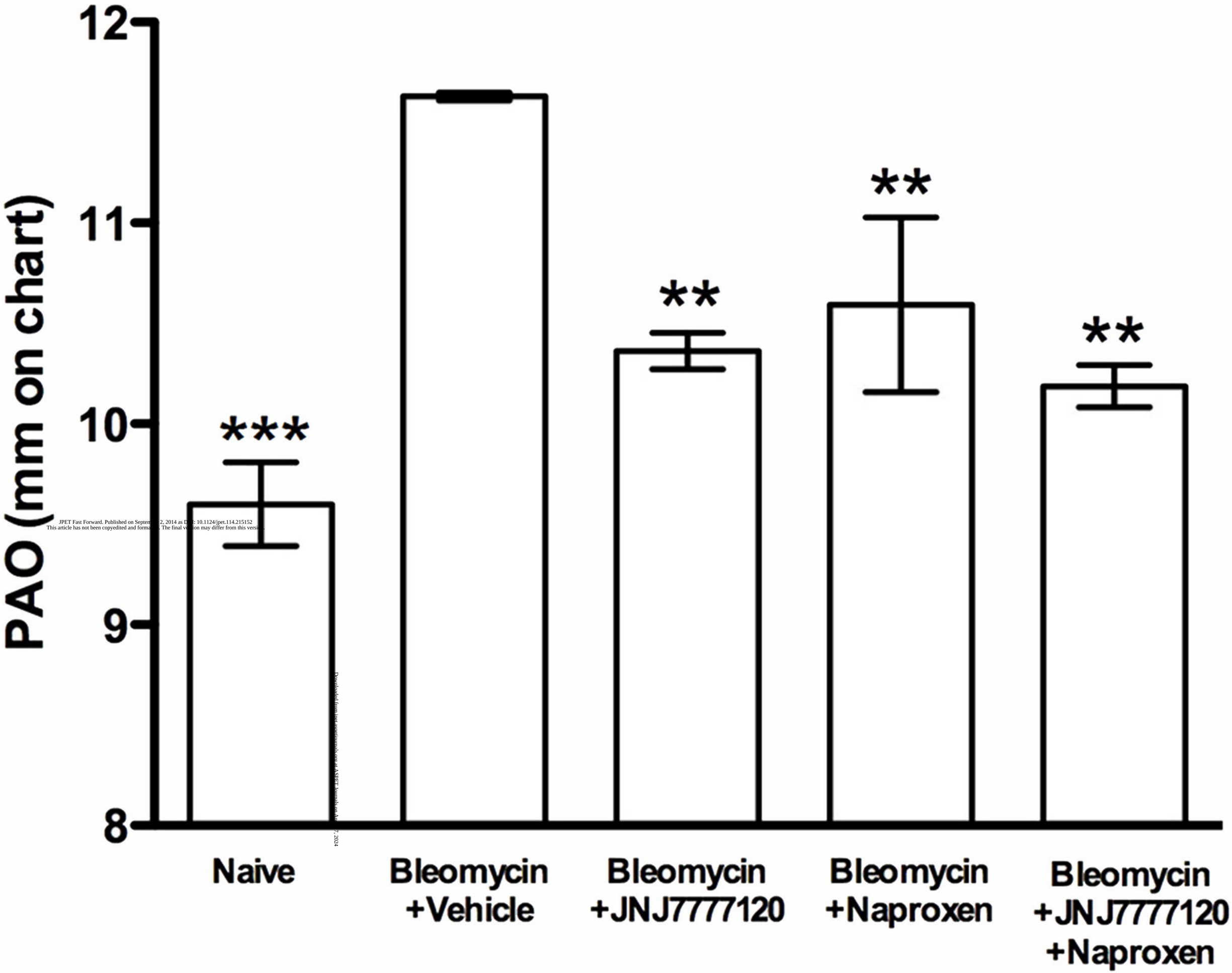

Fig. 2

A

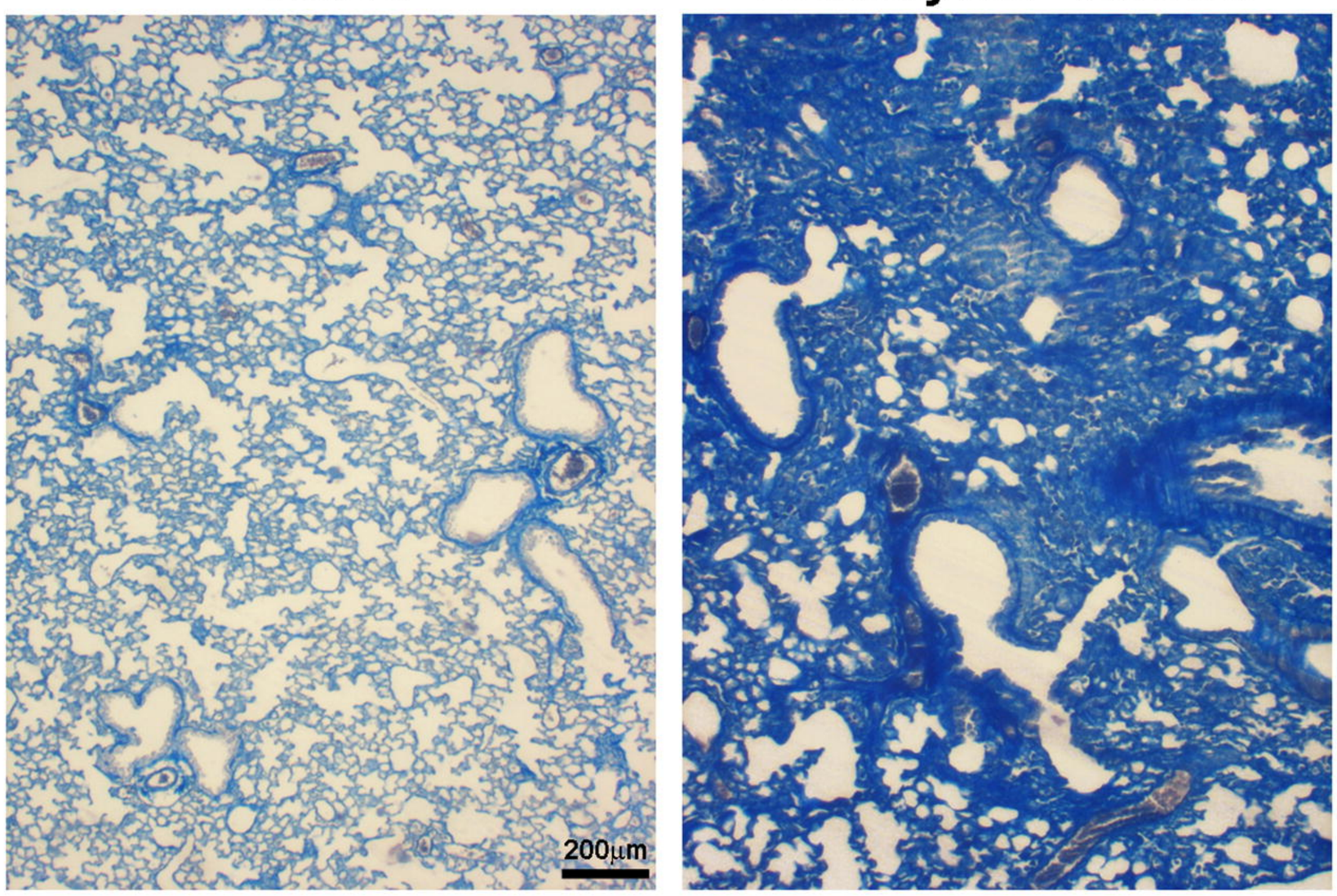

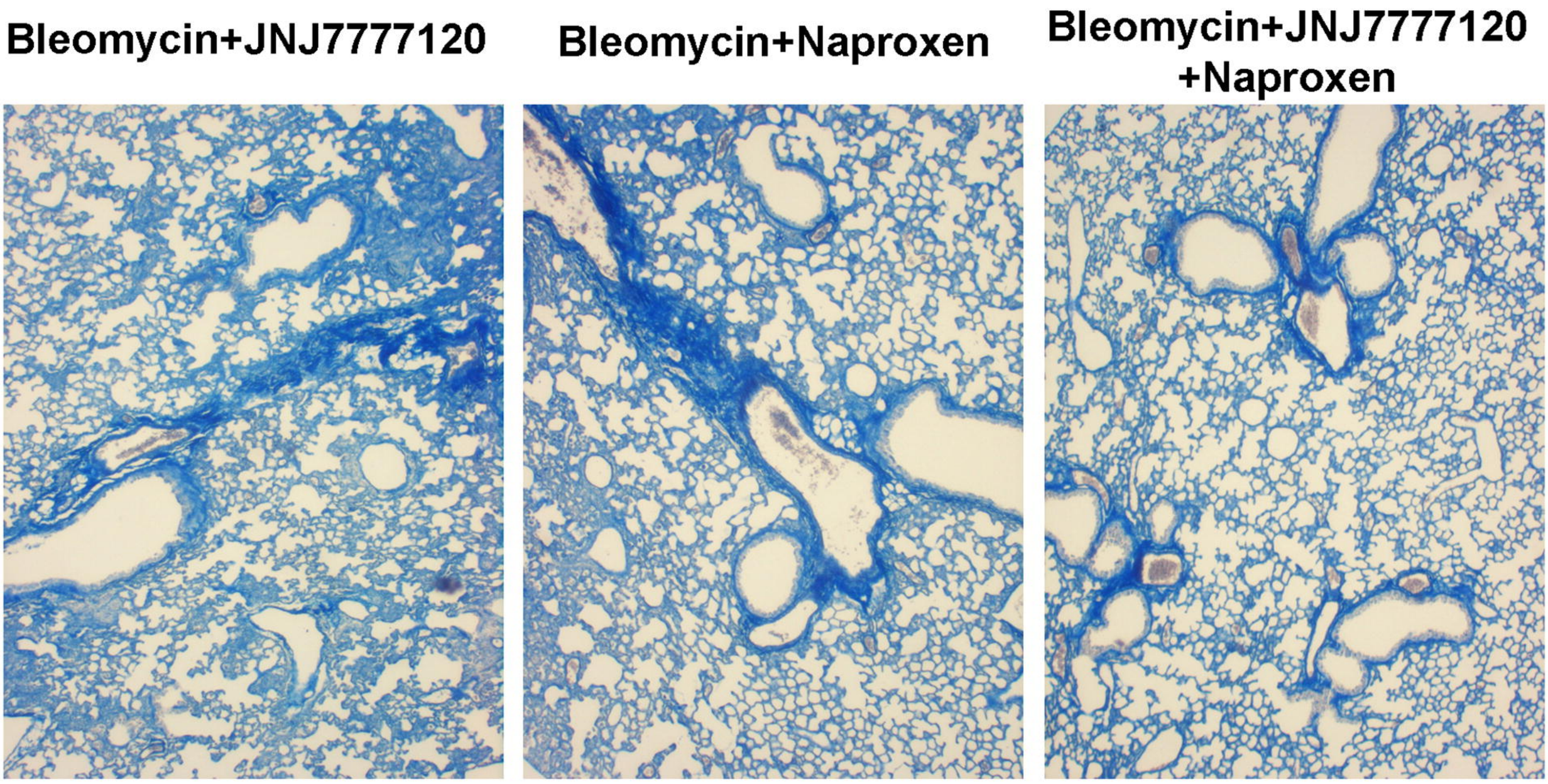

B

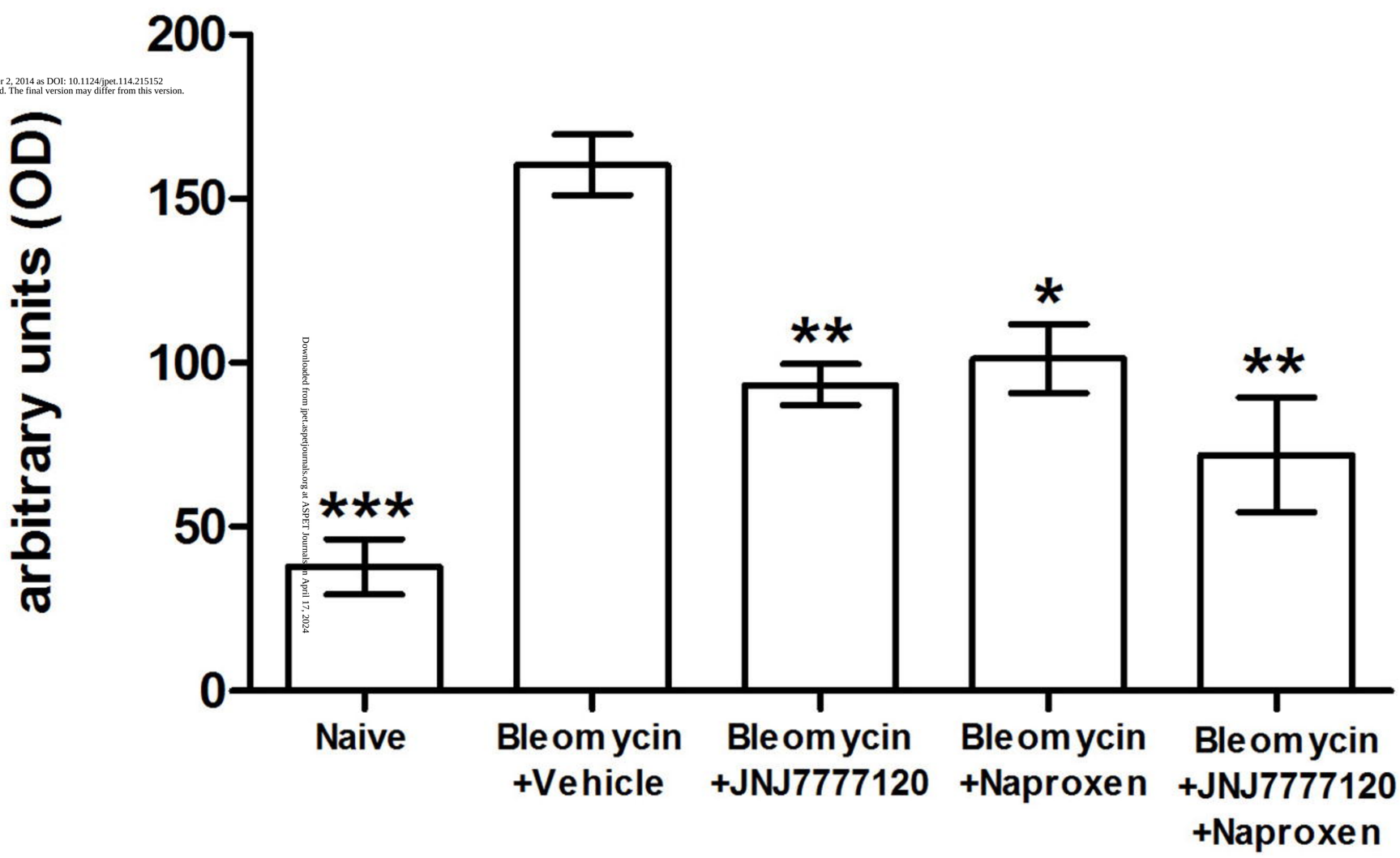

JPET Fast Forward. Published on September 2, 2014 as DOI: 10.1124/jpet.114.215152
This article has not been copyedited and formatted. The final version may differ from this version.

Fig. 3

A

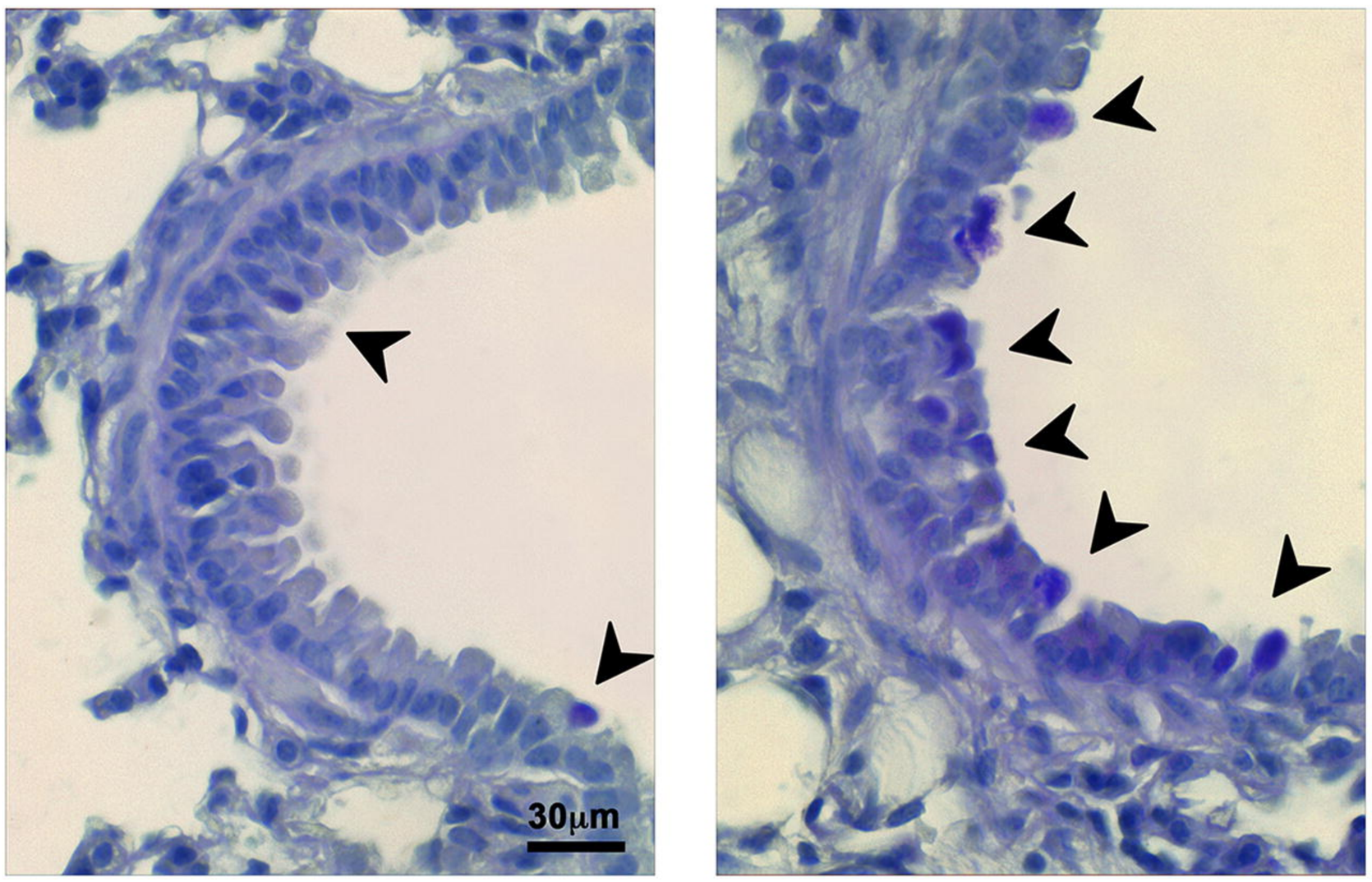

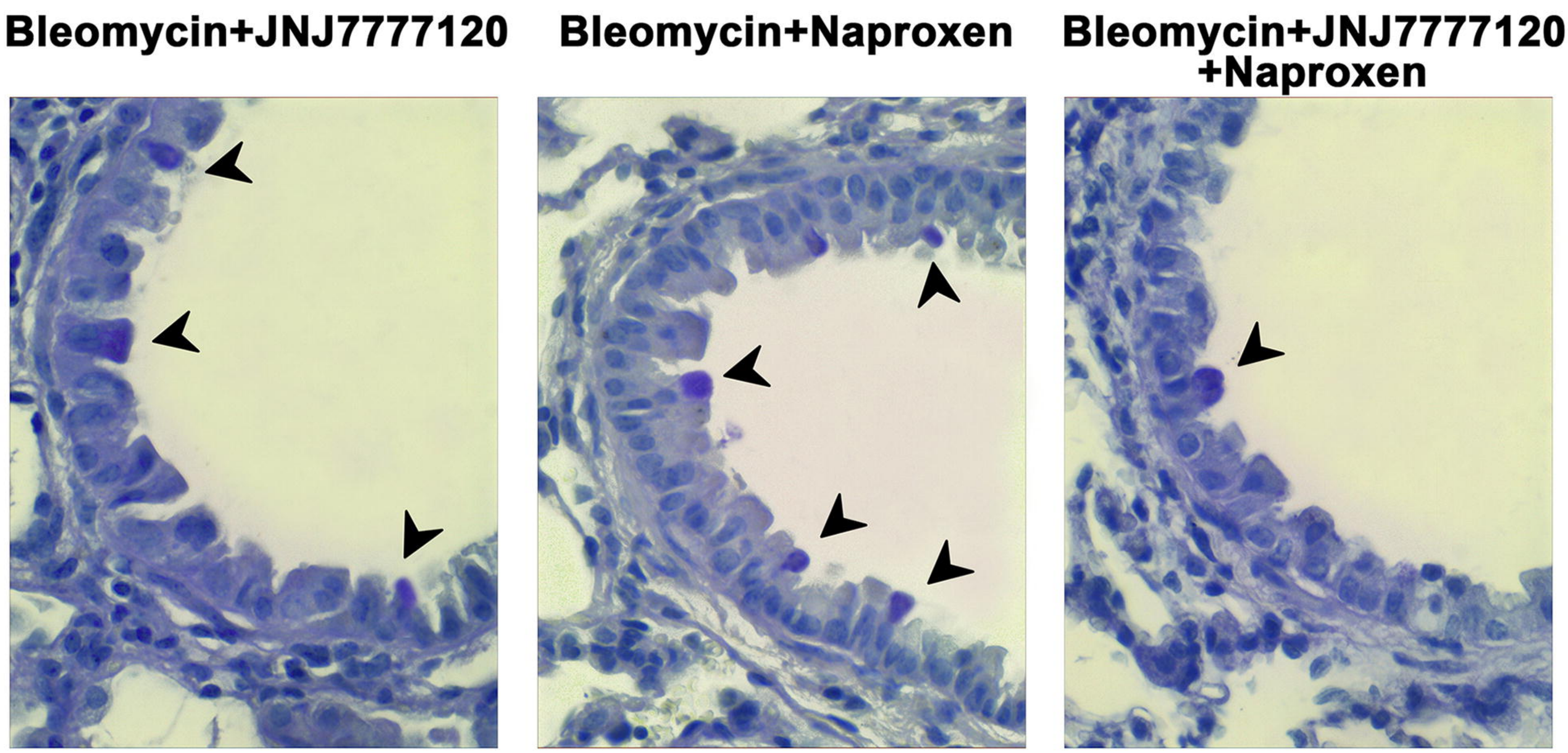

B

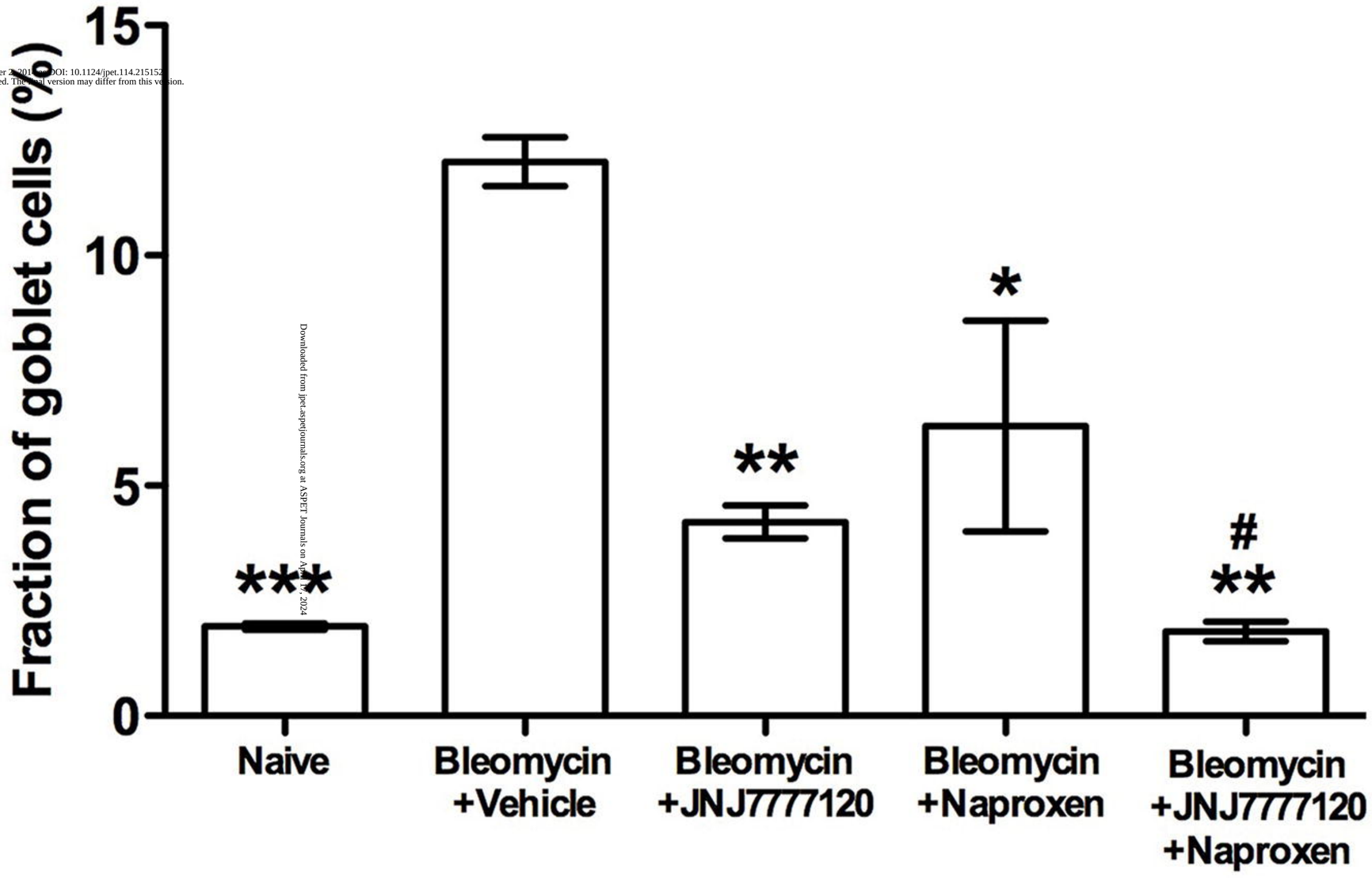

JPET Fast Forward. Published on September 2, 2015 as DOI: 10.1124/jpet.114.215152
This article has not been copyedited and formatted. The final version may differ from this version.

Fig. 4

A

Naive

Bleomycin+Vehicle

30μm

Bleomycin+JNJ7777120

Bleomycin+Naproxen

Bleomycin+JNJ7777120 +Naproxen

B

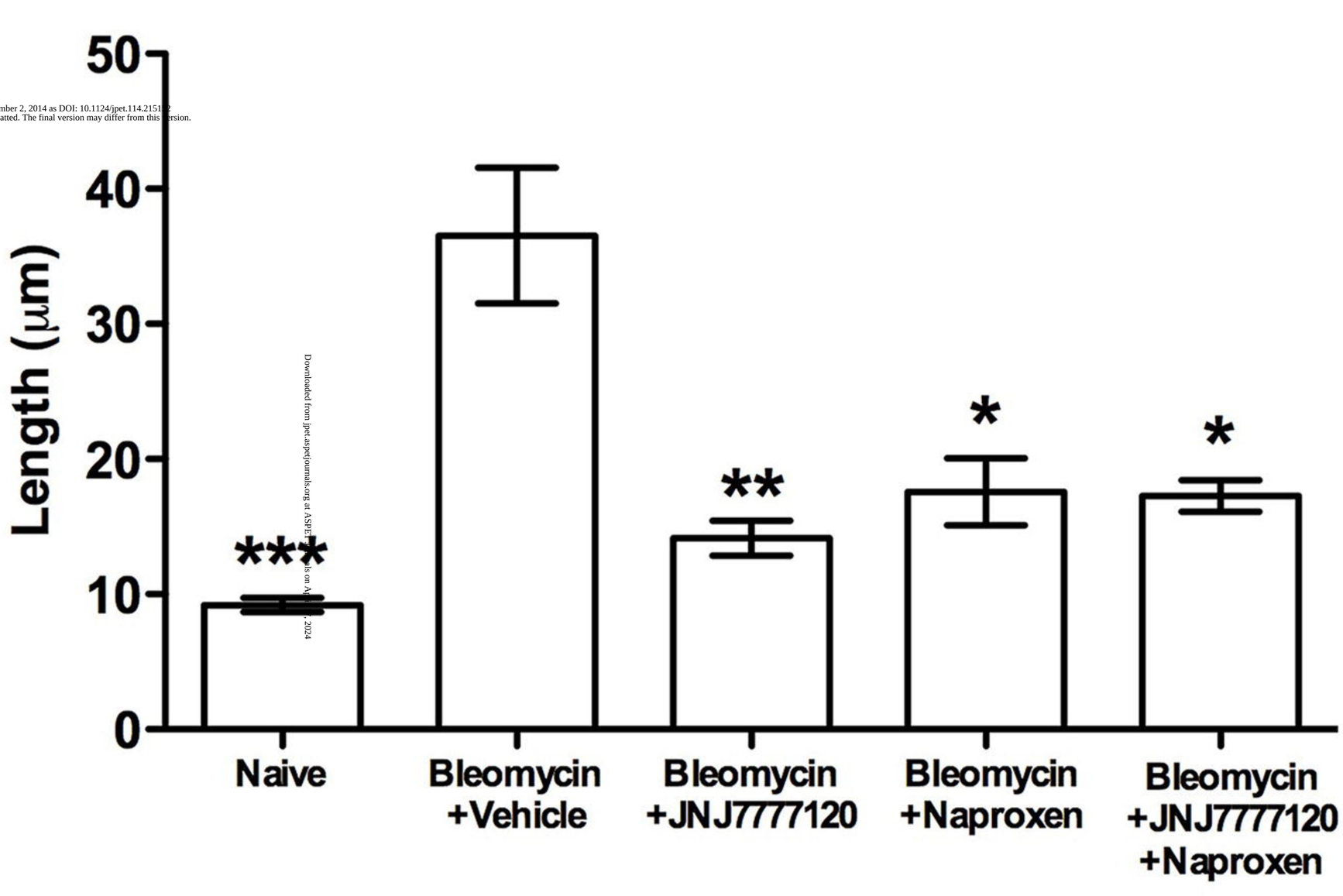

JPET Fast Forward. Published on September 2, 2014 as DOI: 10.1124/jpet.114.215152
This article has not been copyedited and formatted. The final version may differ from this version.

Fig. 5

A

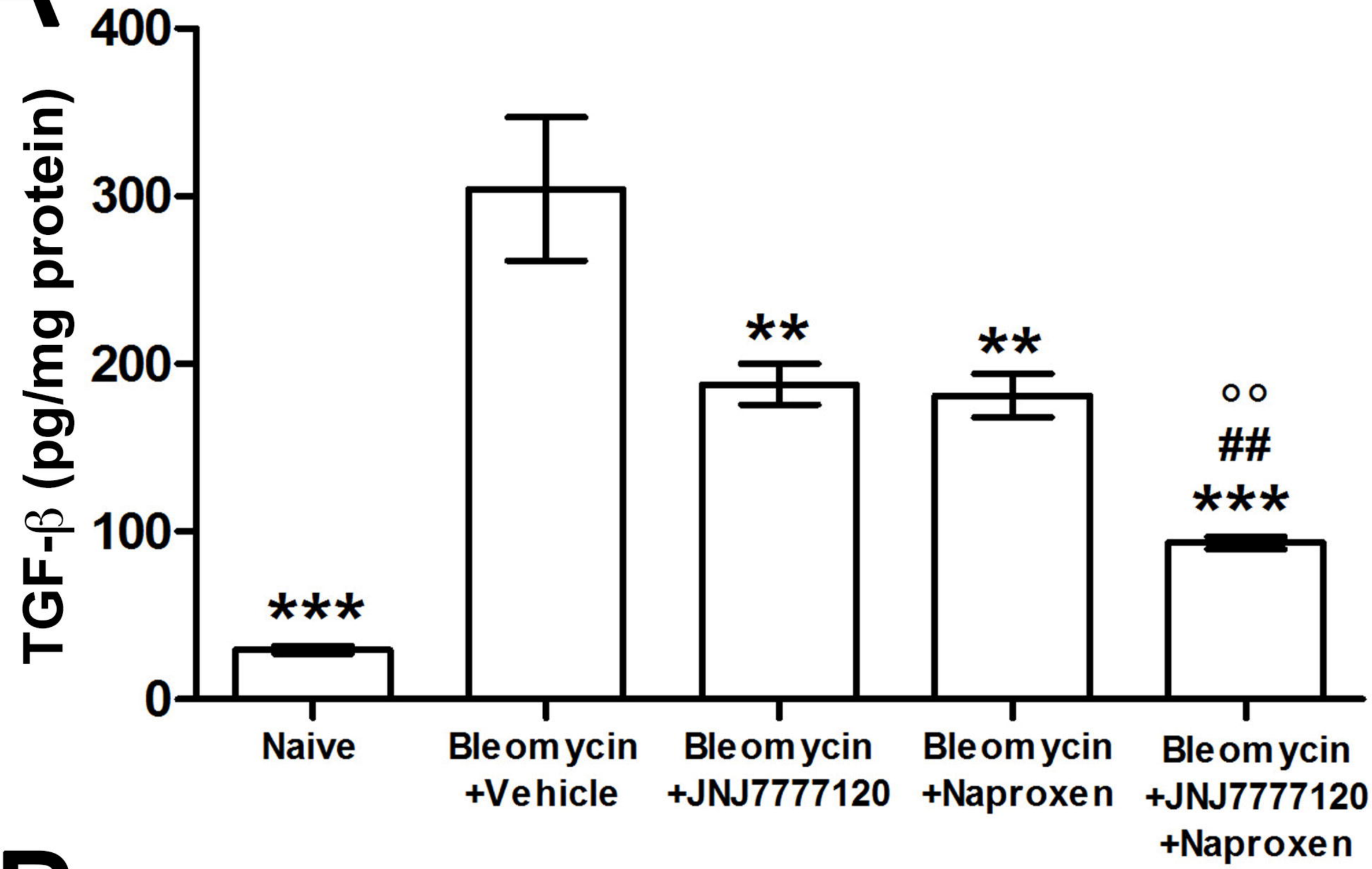

B

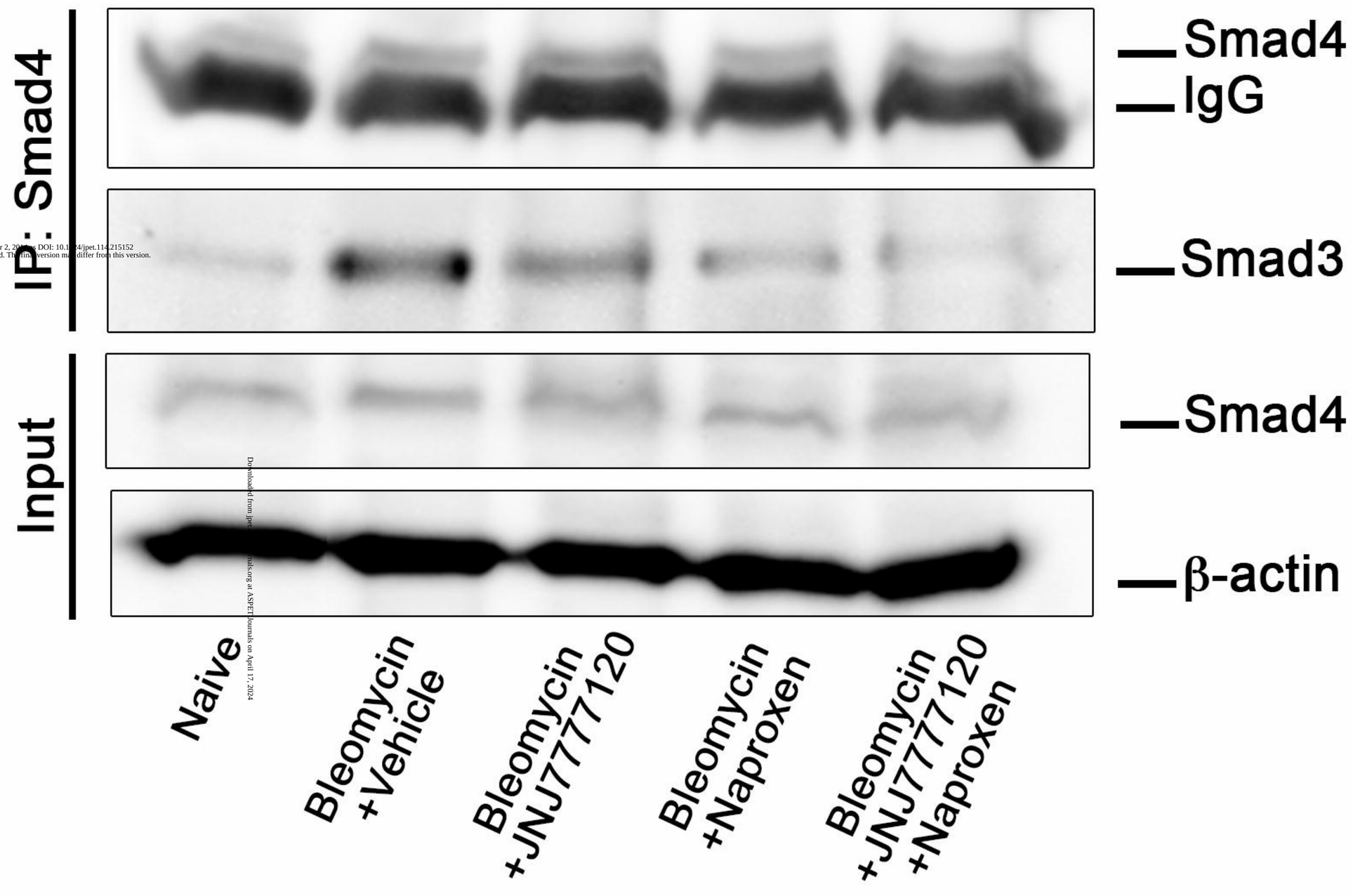

Fig. 6

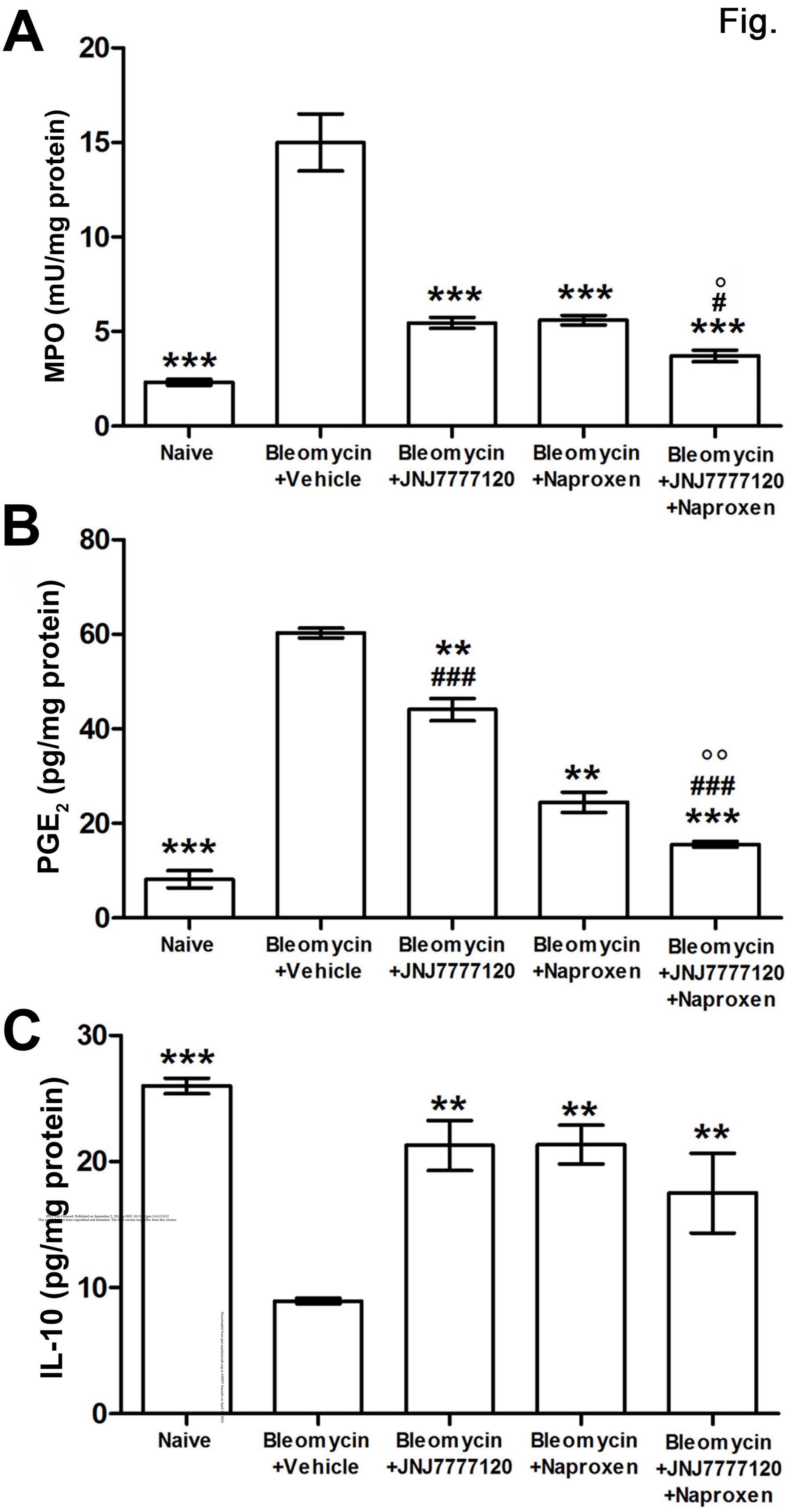

Fig. 7